Low-Order Thermoacoustic Analysis of Real Engines

Symposium on Thermoacoustics in Combustion: Industry meets Academia (SoTiC 2021)
Sept. 6 - Sept. 10, 2021
Munich, Germany
Paper No.: 8496

Abhijeet Badhe[1], Charlélie Laurent[1], Corentin Lapeyre[1] and Franck Nicoud[2]

Abstract

This article illustrates the capability of the recently introduced low-order acoustic-network modeling (LOM) approach *(Laurent et al., Combust. Flame, vol. 206, 2019)* based on the 'generalized modal-expansions' and the 'state-space' framework to study thermoacoustic combustion instabilities in complex realistic configurations under the assumption of zero-Mach mean flow conditions. The acoustics modeling is essentially an improved and generalized version of the classical modal expansions (Galerkin series) technique. Here, one can use as the basis functions either an over-complete set of acoustic eigenmodes (called an Over-Complete (OC) Frame) or a simple orthogonal (OB) basis as has been the norm so far. The former, where deemed necessary, offers enhanced convergence, correct representation of acoustic variables at the interfaces of the subdomains in the network fixing issues such as Gibbs oscillations, and at the same time, presents the opportunity for interconnecting subdomains with 1D/2D/3D acoustics and even modeling advanced features such as complex boundary impedances and multi-perforated liners *(Laurent et al., J Comp. Phy., vol. 428, 2021)*. The potential of the tool is illustrated by performing a linear stability analysis of a real SAFRAN aeronautical engine combustor with twenty 3D quasi-compact flames while keeping all the geometrical complexities intact. The results are similar to those obtained by a 3D finite element based Helmholtz solver but with CPU-time significantly lower (by 3 orders of magnitude). These observations suggest the feasibility of exploiting the tool for extensive parametric studies directly on industrially relevant configurations.

Keywords

Acoustic Network tool, Low-Order Modeling (LOM), Modal Expansions, Galerkin Series, State-Space, Linear Stability Analysis, Annular Engine, Azimuthal Instabilities

Introduction

A new low-order acoustic-network modeling (LOM) tool for studying thermoacoustic combustion instabilities in complex realistic configurations, under zero-Mach mean flow conditions, is under development at CERFACS. It is based on the *state-space* framework and *generalized modal expansions*[1,2].

High fidelity LES is very powerful in predicting instabilities, but cannot be relied upon as a standalone design tool due to its extreme computational costs[3–5]. This is especially true in the process of determining optimal passive control strategies which require generating stability maps and an understanding of the system behavior over a wide parameter space owing to the sensitivity of instabilities to design and operating conditions[6,7]. Therefore, simplified theoretical and reduced-order (ROM) or low-order (LOM) acoustic tools, such as FEM based Helmholtz solver[8] and network-models[9–16], are frequently used in practice.

Network tools solve the thermoacoustic problems based on quasi-analytical techniques wherein a complex configuration to be analyzed is decomposed into simple acoustic sub-domains that are connected/coupled to construct a network. They can be broadly classified based on the spatial description of the acoustics[17] in the sub-domains as Characteristic Wave-based (Riemann Invariants)[9,11,12] or Modal expansion (Galerkin series)[1,14,18,19] models. While the former is mostly limited to 1D longitudinal geometries and idealized annulus-like geometries, the latter allows considering multi-dimensional 2D/3D acoustics as well. Recently, some research groups[20,21] have employed both approaches simultaneously to study nonlinear modal interactions in idealized annular combustors.

Thermoacoustic Network Modeling

In this new tool, named **STORM** (**St**ate-Space **R**educed **O**rdered **M**odeling), the acoustics modeling is based on the idea of modal expansions. The acoustic network representing the system to be analyzed is built by dividing them into network objects: simpler *geometrical* subdomains, *connection* elements, *impedance* and *flame* elements. The subdomains can be trivial geometries with 1D/2D acoustics or even arbitrary shapes with 3D acoustics. Connection elements are required to couple subdomains in the network by imposing appropriate physical conditions at the interfaces. The *state-space* framework adopted in the thermoacoustics community by many[12,13,22–24] in the context of acoustic network modeling has been employed to allow convenient interconnections between different network objects.

[1] CERFACS, 42 Ave Gaspard Coriolis, Toulouse, FRANCE 31057
[2] IMAG, Univ. Montpellier, CNRS, Montpellier, FRANCE 34090

Corresponding author:
Abhijeet Badhe
Email: badhe@cerfacs.fr

Over-Complete Frame Modal Expansion

In the modal-expansions method, the thermoacoustic pressure field in each *geometrical* sub-domain of the network is expressed as a linear combination or series expansion of natural acoustic eigenmodes of that particular subdomain (the basis functions),

$$p(\vec{x},t) = \sum_{n=1}^{N} \dot{\Gamma}_n(t)\phi_n(\vec{x}) = \dot{\mathbf{\Gamma}}^T(t)\boldsymbol{\phi}(\vec{x}) \tag{1}$$

where N is a finite number of natural eigenmodes, $\phi_n(\vec{x})$ denote the basis functions and $\dot{\Gamma}_n(t)$ are the corresponding modal amplitudes or coefficients. Note that in the above equation, the natural modes are known apriori as analytical or numerical solutions to homogeneous Helmholtz equation (without flame source term, non-trivial boundary impedances, etc.) for a given subdomain. The modal amplitudes are therefore the unknown variables to be determined. They are subject to the influence of boundary conditions imposed by neighboring subdomains, and to the volumetric forcing exerted by active flames if present. The modal basis represents the spatial structure of the acoustic pressure field while the modal amplitudes determine its temporal evolution. The acoustic velocity field in the subdomain can also be constructed from the gradient of the modal basis as follows:

$$\vec{u}(\vec{x},t) = -\frac{1}{\rho_0}\sum_{n=1}^{N}\Gamma_n(t)\vec{\nabla}\phi_n(\vec{x}) = -\frac{1}{\rho_0}\mathbf{\Gamma}^T(t)\vec{\boldsymbol{\nabla}}\boldsymbol{\phi}(\vec{x}) \tag{2}$$

Laurent et al.[1] improved and generalized the classical modal expansions (Galerkin series) technique. Most previous studies based on modeling of acoustics through Galerkin series employed *rigid-wall* natural eigenmodes as an orthogonal basis describing the thermoacoustic pressure field . However in this recently proposed approach, one can use as the basis functions either an over-complete set of acoustic eigenmodes (called an *Over-Complete (OC) Frame*) or a simple *Orthogonal Basis (OB)* as has been the norm so far. The former, where deemed necessary, offers enhanced convergence, correct representation of acoustic variables at the interfaces of the subdomains of the network, and fix issues such as Gibbs oscillations. An *Over-Complete Frame* can mathematically be described as a union of two sets of orthogonal bases verifying different acoustic BCs. In practice, a convenient way to build a frame is by collating rigid-wall (u'=0) and pressure release (p'=0) natural eigenmodes. The second family verifies at least one p'=0 boundary which is usually located at the connection boundary between two subdomains. Modal Expansion on a Frame eventually relaxes (or unconstrains) the u'=0 (and p'=0) conditions owing to the constituent orthogonal bases, thus facilitating the correct representation of acoustic variables at the interface. Consequently, this concept has also proved useful in devising the so-called *Surface Spectral Connections* methodology[2] to facilitate coupling between 2D or 3D acoustic subdomains characterized by topologically large and curved boundary interfaces. These spectral connects also offer the possibility to impose Rayleigh conductivity or complex impedance, to model it as multi-perforated liner or complex-impedance boundary, thanks to frame modal expansions.

The thermoacoustic pressure field for a given subdomain Ω_i i.e. solutions of inhomogeneous Helmholtz equation are sought by projecting it onto the OC Frame or the OB basis through the Galerkin projection process detailed rigorously in the paper[1]. It yields a system of dynamic equations that govern the modal amplitudes in Eq.(1 and 2) as follows:

$$\begin{aligned}\ddot{\Gamma}_n(t) = &-\delta\dot{\Gamma}_n(t) - \omega_n^2\Gamma_n(t) \\ &+ \sum_{m=1}^{M_S}\iint_{S_{ci}^{(m)}} \rho_0 c_0^2\Big(\varphi^{S_{ci}^{(m)}}(\vec{x}_s,t)\left[\mathbf{\Lambda^{-1}}\boldsymbol{\nabla_s}\boldsymbol{\phi}(\vec{x}_s)\right]_n \\ &\quad - u_s^{S_{ci}^{(m)}}(\vec{x}_s,t)\left[\mathbf{\Lambda^{-1}}\boldsymbol{\phi}(\vec{x}_s)\right]_n\Big)d^2\vec{x}_s \\ &\quad + \sum_{l=1}^{M_H}(\gamma-1)Q_l(t)\left[\mathbf{\Lambda}^{-1}\left\langle\boldsymbol{\phi},\mathcal{H}_i^l(\vec{x})\right\rangle\right]_n\end{aligned} \tag{3}$$

where subdomain Ω_i is connected to $m=1$ to M_S adjacent subdomains over $S_{ci}^{(m)}$ connection boundaries. In the right hand side of the Eq.(3) the surface integrals, over each $S_{ci}^{(m)}$, are boundary source terms representing the acoustic potential $\varphi^{S_{ci}^{(m)}}(\vec{x}_s,t)$ and acoustic velocity $u_s^{S_{ci}^{(m)}}(\vec{x}_s,t)$ forcing on Ω_i from adjacent subdomains in the network respectively. $\mathbf{\Lambda}_{nm} = \langle\phi_n,\phi_m\rangle = \iiint \phi_n(\vec{x})\phi_m(\vec{x})d^3\vec{x}$, is the *Gram matrix* whose elements are the inner products between the OC frame or OB basis modes. In case of OB, $\mathbf{\Lambda}$ is a diagonal matrix since $\langle\phi_n,\phi_m\rangle = 0$ for $n \neq m$ due to orthogonality. $\boldsymbol{\nabla_s}\boldsymbol{\phi}(\vec{x}_s)$ is a column vector containing the normal gradients of the OC/OB modes on the connection boundaries $S_{ci}^{(m)}$. In Eq.(3, $[\ ]_n$ denotes the n^{th} component of a column vector. A subdomain Ω_i can also have none or $l=1$ to M_H number of heat sources (or flames) within it and the last term is this volume source term due to flames. $\left\langle\boldsymbol{\phi},\mathcal{H}_i^l(\vec{x})\right\rangle$ a column vector containing the scalar products, thus representing the projection of the physical flame shape $\mathcal{H}_i^l(\vec{x})$ on the OC frame or OB basis and $Q_l(t)$ is the global fluctuating heat release rate.

Note that it is not necessary to use a modal frame in the expansion of all subdomains at all times and the choice is based on geometrical and physical considerations, as would be pointed out in the subsequent examples. Under many situations, a simple orthogonal basis is sufficient. In such a case, the frame $\phi_n(\vec{x})$ could be replaced by an orthogonal basis, and the above system of equations (Eq.3) specific to frames[1,2] are still applicable thanks to their generality. They simply reduce to the classical Galerkin projection equations due to the orthogonality of basis modes.

Discussing the implications and underlying challenges associated with frame modal expansions is beyond the scope of this article. The key difficulties are linked to the over-complete nature of the frame leading to: i) numerically ill-conditioned Gram matrix and its inversion, ii) apparition of spurious unphysical components in the resolution of the system network. All these issues are required to be addressed meticulously for the success of the frame expansion method and they are detailed in the references[1,2].

State-Space and Acoustic Network Representation

The dynamical system of subdomain Ω_i in Eq.(3) is recast into a state-space sub-model which is given as follows:

$$\begin{aligned}\dot{\mathbf{X}}^{(i)}(t) &= \mathbf{A}^{(i)}\mathbf{X}^{(i)}(t) + \mathbf{B}^{(i)}\mathbf{U}^{(i)}(t)\\ \mathbf{Y}^{(i)}(t) &= \mathbf{C}^{(i)}\mathbf{X}^{(i)}(t) + \mathbf{D}^{(i)}\mathbf{U}^{(i)}(t)\end{aligned} \tag{4}$$

where $\mathbf{X}$ is the state-vector containing the dynamical variables that completely describe the state of the subsystem - here the modal amplitudes $\dot{\Gamma}_n(t)$ and $\Gamma_n(t)$. $\mathbf{A}$ is the dynamics matrix which is characteristic of subdomain Ω_i's geometry and physical conditions. $\mathbf{B}$ and $\mathbf{U}$ are the input the matrix and vector respectively that includes information of forcing terms acting on the subdomain Ω_i. Therefore, the first line of Eq.(4) is dynamics equations governing the temporal evolution of the state-variables in the subsystem (i), under the forcing from the rest of the network. On the contrary, the second line of Eq.(4) is used to compute the forcing applied by the subsystem (i) onto other elements in the network.

Such state-space sub-models are generated for all the subdomains and other objects (connection elements, flames, impedances) in the network. They all are eventually coupled together to obtain the *global state-space model of the system* by recursively applying the so-called Redheffer product that relates the input-output matrices/vectors of the state-space submodels interacting with each other[1]. Consequently, a closed-loop coupling is established between all the subsystems leading to the global state-space dynamics equation

$$\dot{\mathbf{X}} = \mathbf{A}\mathbf{X}(t) + \mathbf{B}\mathbf{U}(t) \tag{5}$$

where $\mathbf{B}$ and $\mathbf{U}(t)$ are global input matrix and vector which is typically zero unless there is some *external* forcing acting on the full system, for eg. an external loudspeaker.

The global state-space model can then be solved in time-domain to study the system-level dynamics or in frequency-domain by finding the eigen frequencies and eigenvectors of global dynamics matrix $\mathbf{A}$ to obtain the eigenmodes of the full system and their stability information.

Surface Spectral Connections

This section briefly describes the working principle of the methodology devised to facilitate coupling between network subdomains with 2D or 3D acoustics over topologically large and curved boundary interfaces. These spectral connections also provide an opportunity to impose Rayleigh conductivity or complex impedance on the interface to model it as a multi-perforated liner or complex-impedance boundary, and was the topic of our recently published article[2].

Indeed acoustic variables are uniform in the transverse direction in 1D subdomains by definition, and they only have a longitudinal spatial dependence. Therefore in configurations with acoustic networks made of 1D subdomains, they make *point connections* with others. For eg: narrow 1D burners ducts connecting with a combustion chamber with 1D/2D/3D acoustics. However, connections between 2D-2D (or 2D-3D) and 3D-3D subdomains in a network would constitute *line-connection* and *surface-connection* respectively. For a given subdomain Ω_i, the surface integrals in the boundary acoustic forcing terms in the system in Eq.(3) simplify for point connections to the variable values at the boundary. Evaluation of these surface integrals in the case of multi-dimensional *surface- (or line-) connections* and was the key challenge addressed in this methodology[2].

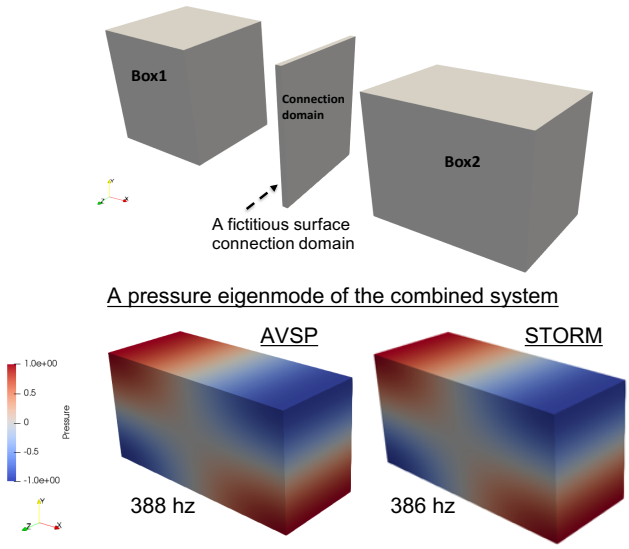

Figure 1. Two 3D cavities connected to each other via a surface spectral connection in STORM. A natural acoustic pressure eigenmode of the combined system in comparison to that from Helmholtz solver AVSP[8].

One approach, initially examined, was to *spatially discretize* the boundary surface into a smaller number of surface elements such that the variables could be considered uniform over each of them, thus leading to a *piece-wise approximation* of the surface integrals. This approach did work in the case of simple subdomains for which frames are defined analytically. However, numerical issues and inconsistent results were encountered in cases where subdomain frames were numerically generated from a FEM-based Helmholtz solver. Besides, deciding upon the location of the connection boundaries while decomposing a complex system to build the acoustic network, and the number of elements on such surfaces isn't straightforward. To overcome these challenges, the current methodology relying on *spectral discretization* was developed.

The core working principle of surface spectral connects is touched upon next with help of a couple of simple examples. An analogous explanation would apply to line spectral connections. Consider a simple acoustic network of two 3D subdomains - Box1 (say subdomain Ω_i) and Box2 (subdomain Ω_j) as shown in Fig. (1), that are to be coupled together to compute the natural acoustic eigenmodes of the combined system. For doing so, a 3D-3D surface spectral connection element is defined for the acoustic network by creating a *fictitious*, thin shell-like (quasi-2D) connection domain (or control volume) (Ω_{sc}) as in Fig.(1)), that is topologically identical in shape and enclosing the connection interface i.e. boundaries S_{c_i} and S_{c_j} of subdomains Ω_i and Ω_j respectively. Note that the subdomain boundaries, and thus the connection domain, could be arbitrarily curved shaped too.

Curvilinear Helmholtz Equations

Starting from linearized Euler equations (LEE), *curvilinear Helmholtz equation* are derived[2] for the fictitious connection domain Ω_{sc} in a spatial curvilinear coordinate system: (α, β, ξ), where (α, β) are two tangential directions and ξ the normal direction of the connection boundaries S_{c_i} and S_{c_j}. The equations are averaged along the ξ-direction, under the limit that thickness of Ω_{sc}, $L_{\mathscr{D}} \to 0$. They are expressed in terms of ξ-*averaged* acoustic potential $\bar{\varphi}(\alpha, \beta, t)$ and normal velocity $\bar{u}_\xi(\alpha, \beta, t)$. The equations are also embedded with appropriate *coupling conditions* which could be simple acoustic pressure and flux continuity (as for the case in Fig.(1)) or complex impedance or conductivity. For instance, the Howe's model defining Rayleigh conductivity of multi-perforated plates is presented in the case depicted in Fig.(2).

The *inhomogeneous* curvilinear Helmholtz and the accompanying linearized momentum equations completely describe the acoustics in connection domain (Ω_{sc}) based upon pressure and normal acoustic velocity on boundaries S_{c_i} and S_{c_j}, and essentially impose the desired coupling condition between the two subdomains.

Surface Modal Expansion

To solve the above curvilinear Helmholtz equation along with the momentum equation, and to generate a state-space submodel for the fictitious Ω_{sc} domain representing a STORM network connection element, the *surface modal expansion* is introduced[2]. The ξ-averaged acoustic variables $\bar{\varphi}(\alpha, \beta, t)$ and $\bar{u}_\xi(\alpha, \beta, t)$ in the connection domain are expanded over an *orthogonal basis* of natural surface eigenmodes as follows:

$$\begin{aligned}\overline{\varphi}(\alpha,\beta,t) &= \sum_{k=1}^{K_s} \nu_k(t)\mathscr{K}_k(\alpha,\beta) = \boldsymbol{\nu}^T(t)\boldsymbol{\mathscr{K}}(\vec{x}_s)\\ \overline{u}_\xi(\alpha,\beta,t) &= \sum_{k=1}^{K_s} \mu_k(t)\mathscr{K}_k(\alpha,\beta) = \boldsymbol{\mu}^T(t)\boldsymbol{\mathscr{K}}(\vec{x}_s)\end{aligned} \quad (6)$$

where the 2D surface eigenmodes basis ($\boldsymbol{\mathscr{K}}(\vec{x}_s)$) is determined apriori from analytical or numerical solutions of *homogeneous* curvilinear Helmholtz equation over the connection domain (Ω_{sc}). The surface basis eigenmodes follow the 2D surface inner product $(f|g) = \iint_{S_{c_i}} f(\vec{x}_s)g(\vec{x}_s)d\vec{x}_s$ and the L-2 squared norm of the basis surface eignemodes are noted as $\lambda_k = (\mathscr{K}_k|\mathscr{K}_k)$.

The classical Galerkin expansion procedure is replicated by injecting the Eq.(6) into the *inhomogeneous curvilinear Helmholtz and momentum* equations described in the previous subsection. In addition, the source terms in those equations - acoustic pressure and velocity on connections boundaries S_{c_i} and S_{c_j}, are substituted from *frame expansions* in subdomains Ω_i and Ω_j, i.e. Eq.(1) and Eq.(2). Subsequently , the following dynamical system of equations is obtained that governs the values of the *surface modal amplitudes* in Eq.(6). This system can be converted into a MIMO state-space submodel[2] representing the surface spectral connection element in the network coupling the two 3D subdomains.

$$\begin{aligned}&\ddot{v}_k(t) + \omega_k^2 v_k(t) = \\ &\quad -\frac{\overline{c_0}^2}{\lambda_k L_{\mathscr{D}}}\left[s_i \sum_{n=1}^{N^{(i)}} -\frac{1}{\rho_0^{(i)}}\left(\nabla_s\phi_n^{(i)} \mid \mathscr{K}_k\right)\Gamma_n^{(i)}(t)\right.\\ &\qquad \left. - s_j \sum_{n=1}^{N^{(j)}} -\frac{1}{\rho_0^{(j)}}\left(\nabla_s\phi_n^{(j)} \mid \mathscr{K}_k\right)\Gamma_n^{(j)}(t)\right]\end{aligned} \quad (7)$$

$$\begin{aligned}&\dot{\mu}_k(t) = \\ &\quad \frac{1}{\lambda_k L_{\mathscr{D}}\overline{\rho_0}}\left[s_i \sum_{n=1}^{N^{(i)}}\left(\phi_n^{(i)} \mid \mathscr{K}_k\right)\dot{\Gamma}_n^{(i)}(t)\right.\\ &\qquad + s_j \sum_{n=1}^{N^{(j)}}\left(\phi_n^{(j)} \mid \mathscr{K}_k\right)\dot{\Gamma}_n^{(j)}(t)\\ &\qquad \left. + s_i \sum_{n=1}^{N^{(i)}} -\frac{1}{\rho_0^{(i)}}\left(\nabla_s\phi_n^{(i)} \mid \mathscr{K}_k\right) Y_{K_R}\left\{\Gamma_n^{(i)}(t)\right\}\right]\end{aligned} \quad (8)$$

The superscripts $^{(i)}$ and $^{(j)}$ refer to quantities evaluated in subdomains Ω_i, Ω_j of OC frame sizes $N^{(i)}$, $N^{(j)}$ respectively. *The presence of the time-dependent subdomain modal amplitudes $\Gamma_n^{(i)}(t)$, $\dot{\Gamma}_n^{(i)}(t)$, $\Gamma_n^{(j)}(t)$ and $\dot{\Gamma}_n^{(j)}(t)$ in the right-hand side of Eq.(7) and Eq.(8) shows that the connection domain (Ω_{sc}) indeed couples the acoustics in Ω_i to that in Ω_j, and vice versa.* Above in Eq.(8) the last term appears from the Howe's model for Rayleigh conductivity embedded into the equations in form of a single-input-single-output (SISO) state-space model which would be absent for the case in Fig.(1). See[2] for more details and the state-space matrices of the surface spectral connection element.

Finally, the surface modal expansions of Eq.(6) allow the surface integrals in Eq.(3) to be rewritten as:

$$\begin{aligned}&\iint_{s_{ci}^{(m)}} \rho_0 c_0^2 \varphi^{S_{c_i}^{(m)}}(\vec{x}_s,t)\left[\boldsymbol{\Lambda}^{-1}\boldsymbol{\nabla_s\phi}(\vec{x}_s)\right]_n d^2\vec{x}_s = \\ &\qquad \rho_0 c_0^2\left[\boldsymbol{\Lambda}^{-1}\left(\boldsymbol{\nabla_s\phi}|\boldsymbol{\mathscr{K}}^T\right)\right]_{n,*}\boldsymbol{\nu}(t)\end{aligned} \quad (9)$$

$$\begin{aligned}&\iint_{S_{ci}^{(m)}} \rho_0 c_0^2 u_s^{S_{ci}^{(m)}}(\vec{x}_s,t)\left[\boldsymbol{\Lambda}^{-1}\boldsymbol{\phi}(\vec{x}_s)\right]_n d^2\vec{x}_s = \\ &\qquad s_i\rho_0 c_0^2\left[\boldsymbol{\Lambda}^{-1}\left(\boldsymbol{\phi}|\boldsymbol{\mathscr{K}}^T\right)\right]_{n,*}\boldsymbol{\mu}(t)\end{aligned} \quad (10)$$

where $[\ ]_{n,*}$ denotes the entire n^{th} row the a matrix. The surface source terms in Eq. (7)are now evaluated thanks to the surface modal projections $\left(\boldsymbol{\phi}|\boldsymbol{\mathscr{K}}^T\right)$ and $\left(\boldsymbol{\nabla_s\phi}|\boldsymbol{\mathscr{K}}^T\right)$ rather than through simple piecewise approximations.

In another canonical case depicted in Fig.(2), cylindrical and annular cavities separated by a multi-perforated liner are modeled in STORM and validated against AVSP[8,25]. Unlike previous example Fig.(1), the Howe's model is used as the coupling condition that is enforced by the surface spectral connection domain[2] (not shown in Fig.(2)). The acoustic damping effect induced by the liner is captured fairly well in

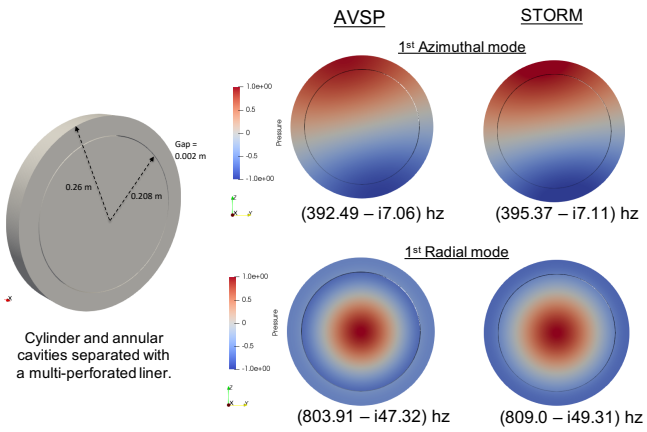

Figure 2. Surface spectral connections for modeling multi-perforated liner between the cylindrical and annular cavities. Two eigenmodes of the system, their frequencies and growth rate. Note that the thin surface connection domain in between the subdomains is not shown.

STORM as highlighted from a couple of system eigenmodes and their negative growth rates.

In summary, a network including surface spectral connections can be viewed as a nested and coupled modal expansion (Galerkin Series) problem. The acoustic field in a subdomain, expanded onto a modal frame, depends on the boundary forcing from adjacent subdomains through a fictitious 2D connection domain imposing coupling conditions; and these boundary source terms are further expanded onto an orthogonal basis of surface eigenmodes. The surface source terms evaluated based on a finite number of surface eigenmodes imply spectral discretization rather than spatial. Hence the name surface spectral connections!

Linear Stability Analysis of SAFRAN Annular Engine Combustor

One of the main goals behind initiating the development of the tool STORM was to make faster, and computationally cheaper thermoacoustic stability analysis of realistic configurations possible. Most low-order network models available in the literature involve drastic simplifications to geometry. Real engine combustors, on the contrary, include intricate geometrical complexities, multiple cavities, and components such as the chamber, casing, plenum, swirlers, dilution holes, multiperforated liners, upstream compressor diffuser and downstream turbine stages all of them interacting acoustically and thus playing a role in the stability of the engine.

Some previous works based on the state-space framework and classical Galerkin expansions did analyze industrial combustors [13,14,22] in the context of low-order network modeling. The acoustics description however was constrained to be on an orthogonal basis with burners being considered as acoustically compact elements modeled as transfer matrices. Bethke et al. [14], had shown that arbitrarily complex geometries can be incorporated in a thermoacoustic LOM by expanding the pressure onto a set of basis functions computed in a preliminary step thanks to a FEM Helmholtz solver.

Linear stability analysis of a SAFRAN aeronautical engine combustor with STORM is presented in this section and validated with classical FEM-based Helmholtz solver (AVSP)[8] predictions. Two cases are considered: ***1) Case-Z∞:*** Chamber Outlet Acoustic Impedance $Z = \infty$ (rigid-wall) and ***2) Case-Z10:*** Outlet Acoustic Impedance Z=10 (arbitrarily chosen just for demonstration). The second case will demonstrate how an over-complete frame in STORM along with the surface spectral connection method helps model non-trivial acoustic boundary conditions at the chamber outlet. Note that, the multi-perforated combustion chamber walls are not modeled in this example.

While a variety of subdomains 1D/2D/3D could be interconnected to construct an acoustic network in STORM, in this particular case, decomposition of the geometry into subdomains (for eg. combustor, casing, plenum, etc). is not necessary. Therefore the entire geometry with all its intricate details intact is represented by a single *3Dcomplex* subdomain in the network Fig.(4-c) to which 20 discrete flames connect. The modal basis (or frame as necessary) for 3Dcomplex domains of arbitrary shapes are generated numerically from FEM Helmholtz solver[8] by solving computationally faster and cheaper Linear Eigenvalue Problem (LEVP) in the absence of active flames. An advantage of using numerical modal basis/frame is the possibility to account for the inhomogeneous temperature field (or sound speed field) in the combustor.

For the *Case-Z∞* (outlet $Z = \infty$), due to simple Neumann BC at the combustor inlet and outlet, and also since there is *no domain-domain connection*, an orthogonal basis made of N=60 modes is chosen and found to be good enough. $Z = \infty$ is often an approximate BC used for combustors terminated in choked nozzles under the low upstream Mach number.

However for the *Case-Z10* (outlet $Z = 10$), a Frame (N=60) is necessary to model the non-trivial resistive impedance considered at the chamber outlet. The surface spectral connections methodology is employed to impose the impedance condition at the outlet: the combustor 3D subdomain couples with a fictitious surface connection domain as shown in Fig.(3) and *'Outlet Z'* in its network representation in Fig. (4d). The spectral connections framework needs to be slightly adapted since the connection domain couples with only one 3D subdomain. In addition, the impedance condition needs to be embedded in the curvilinear Helmholtz and momentum equations discussed in the previous section. A first-order complex rational function in Eq.(11) for the impedance is assumed and fit (with parameters r and ω_c) to get the desired impedance value, Z=10 in this case.

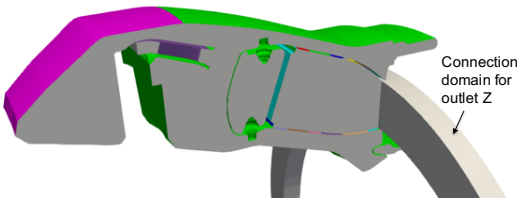

Figure 3. Surface spectral connection domain created to model the chamber outlet impedance.

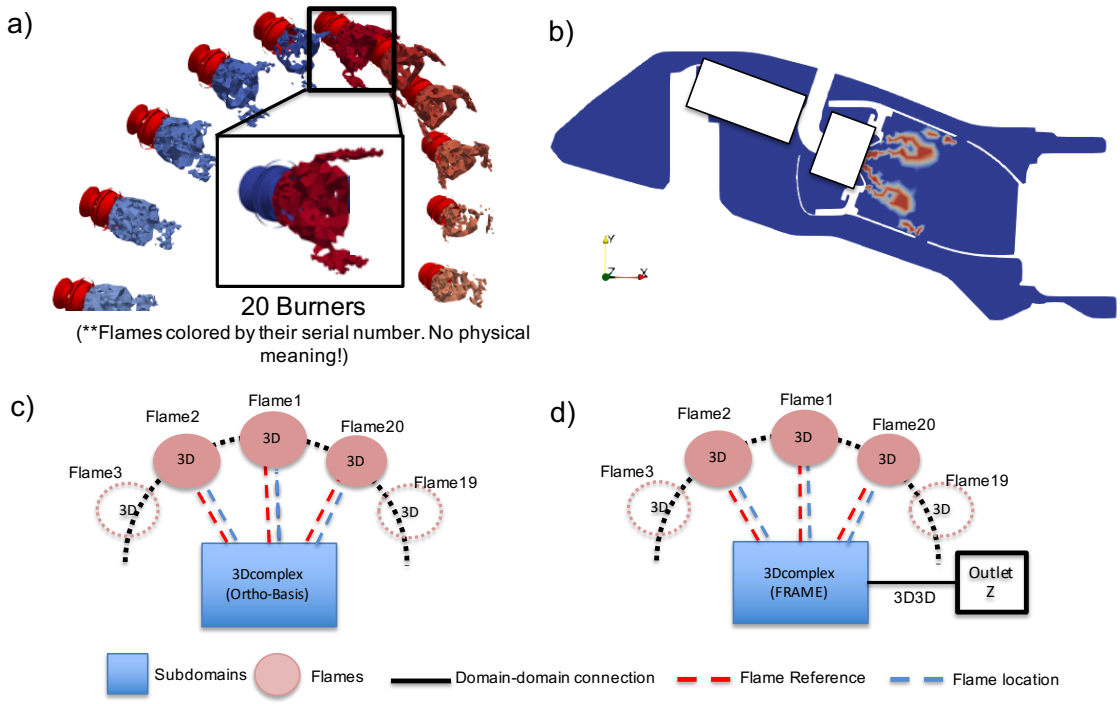

Figure 4. Annular Aeronautical Engine Combustor: a) 20 burners and the mean 3D flame shapes, b) cross-sectional cut of the combustor. An illustrative acoustic-network representation in STORM of two different cases based on chamber outlet impedance: c) ***Case Z=***∞ (i.e. rigid wall) and d) ***Case Z=10***

Table 1. Natural and Thermoacoustic (TA) modes of the annular engine combustor computed from STORM and Helmholtz solver AVSP. Modes with positive imaginary part (growth rate) are unstable modes.

Natural Modes (hz)	**TA Mode**	**STORM (Case-Z∞) (hz)**	**AVSP (Case-Z∞) (hz)**	**STORM (Case-Z10) (hz)**	**AVSP (Case-Z10) (hz)**
308	1	$(292 - 7.7j)$	$(292 - 7.6j)$	$(291 - 14.9j)$	$(291 - 11.6j)$
308	2	$(304 - 17.5j)$	$(304 - 24.8j)$	$(305 - 24.8j)$	$(304 - 21.2j)$
389	3	$(398 + 28.4j)$	$(398 + 27.4j)$	$(398 + 20.3j)$	$(395 + 21.9j)$
497	4	$(494 + 13.9j)$	$(494 + 13.8j)$	$(494 + 3.7j)$	$(492 + 7.9j)$
497	5	$(502 + 15.6j)$	$(501 + 15.4j)$	$(501 + 4.0j)$	$(498 + 8.6j)$

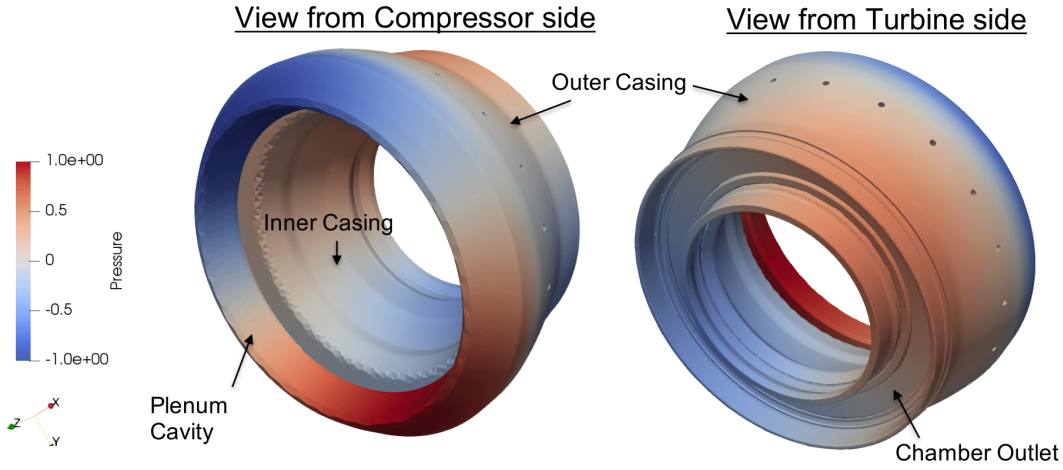

Figure 5. An unstable thermoacoustic mode (TA Mode4 in Tab. 1) of the annular combustor predicted with STORM with a mixed azimuthal-longitudinal structure.

$$Z(j\omega) = \frac{1}{\rho_0 c_0}\frac{\hat{p}(\vec{x},\omega)}{\hat{u}(\vec{x},\omega)} = \frac{1}{r + j\omega/\omega_c} \tag{11}$$

Each 3D flame is represented as a separate flame-element in the STORM network as depicted in Fig.(4). This is done for the sake of modularity and flexibility, and to keep the possibility to study symmetry breaking effects open by modifying the flame response (say due to fuel-staging or using different burners along the annulus). The acoustic response of all the flames is taken identical for the current calculations and is associated with one global constant gain and delay $(n-\tau)$type Flame Transfer Function (FTF) as in Eq.(12). The frequency-domain FTF firstly must be transformed into a time-domain state-space form before it can be included in the network.

$$\frac{\hat{Q}(\omega)}{\bar{Q}} = N\left(\frac{\hat{u}(x_{ref},\omega)}{\bar{u}}\right)e^{-j\omega\tau} \tag{12}$$

This is achieved through an approximation of the exponential term in the FTF as a series of rational functions is realized through a Multi-Pole Expansion:

$$e^{-j\omega\tau} \approx \sum_{k=1}^{M_{PBF}} \frac{-2a_k j\omega}{\omega^2 + 2c_k j\omega - \omega_{0k}^2} \tag{13}$$

where each term in the series is called a Pole-Base-Function (PBF). The coefficients a_k, c_k, ω_{0k} are determined with help of a recursive fitting algorithm proposed by Douasbin et al.[26]. Taking the inverse Fourier transform of this series of PBFs, the state-space form could be derived[1]. The methodology could also be used to fit more generic frequency-dependent FTFs computed from LES or experimental measurements. Alternatively, the Vector Fitting algorithm proposed by Gustavsen et al.[27] and its newer robust versions could be employed for such rational-approximations too.

Computing thermoacoustic modes of the current configuration with the Helmholtz solver AVSP in the presence of active flames and/or nontrivial impedances translates into a Nonlinear Eigenvalue Problem (NLEVP)[8] which require iterative resolution methods (eg: fixed-point-algorithm). The TA modes have to be individually converged by providing an initial guess. This process can become really cumbersome and computationally expensive especially for such large industrial configurations. Note also that often convergence difficulties are encountered, for eg: 1) cases when there is significant drift in frequencies due to very strong flame response, 2) in case of azimuthal modes which always come in pair, 3) when there are many TA modes of the system clustered on the complex-frequency plane, there is no guarantee convergence to each of them would be achieved. There are some promising new approaches proposed by other research groups for efficient and faster computations of thermoacoustic NLEVP problems, for eg: 1) the approach based on contour integration to solve the NLEVP[28], 2) Application of Bloch-Wave theory to configurations with rotational symmetry[29].

STORM performs exceedingly well in this context. It gave the stability of all the TA modes of the annular combustor (equal to the number of basis/frame modes in the expansion) in just one calculation within a few minutes. Table 1 lists the first few TA eigenmodes of the combustor obtained from STORM along with the reference solution from AVSP. The increased damping caused due to the resistive impedance at the outlet is visible in the growth rates of modes for Case-Z10 (outlet impedance Z=10). The pre-processing steps described earlier of computing the natural modes of the system, constructing the numerical basis/frame, and the projection of 20 flames on it, are slightly CPU intensive calculations than the STORM calculation itself. Still, a comparison of total CPU-time required by AVSP for computing the first few TA modes and STORM (including the preprocessing) gave a factor larger than 10^3. Thermoacoustic calculations of a full-scale annular industrial configuration at such a low cost and speed are indeed worth noting.

Conclusions and Outlook

STORM- a low-order acoustic network modeling tool based on the state-space framework and generalized modal expansions for studying thermoacoustic instabilities (under zero-Mach mean flow assumption) in complex realistic configurations has been briefly described. Generalized Modal Expansions[1] is an improved version of the classical Galerkin-series method allowing the use of an overcomplete (OC) frame of acoustic eigenmodes, if needful, in addition to an orthogonal basis (OB). OC frames improve the convergence of the expansion, and yields a precise description of the acoustic field, particularly in networks containing multiple subdomains. In addition it facilitates seamless interconnections between subdomains with 1D/2D/3D acoustics and modeling spatially elaborate complex boundary impedances with *Surface Spectral Connections*[2] methodology.

The capabilities of the tool were highlighted by carrying out the linear stability analysis of a SAFRAN annular engine combustor. The two cases that were analyzed illustrated the flexibility to use classical *orthogonal basis* or *overcomplete frame* as required and the strength of the latter, for example, to model the non-trivial outlet impedance with help of *surface spectral connection* approach. The significant gain in required CPU-time (by 3 orders of magnitude) against Helmholtz solver AVSP and the modularity offered by the network approach, suggests the feasibility of conducting extensive parametric studies directly on complex industrial configurations.

Work-in-progress includes extending the theory and proof-of-concept in[2] for modeling: 1) complex combustor outlet impedances offered by downstream turbine stages for predicting mixed-entropy-acoustic combustion instabilities[30], and 2) industrial multi-perforated liners where some modeling difficulties arise due to the presence of several dilution holes on liner walls. A Python API (Application Programming Interface) is being developed as well to aide in creating and managing complex acoustic networks, and for faster industry deployment of the tool. There is a healthy scope of developing this methodology further into a comprehensive tool for thermoacoustic analysis of combustion systems: inclusion of adjoint methods for systematic optimization and UQ studies[31], nonlinear stability analysis, time-domain simulations, etc.

Acknowledgements

Funding from European Commission under MSCA ITN Project ANNULIGHT (Grant Agreement No. 765998) (https://www.ntnu.edu/annulight) is gratefully acknowledged. The second author thanks the French Ministry of Higher Education, Research and Innovation and the École Normale Supérieure de Paris-Saclay for funding through the CDSN scheme.

References

1. Laurent C, Bauerheim M, Poinsot T et al. A novel modal expansion method for low-order modeling of thermoacoustic instabilities in complex geometries. *Combustion and Flame* 2019; 206: 334–348.
2. Laurent C, Badhe A and Nicoud F. Representing geometrically complex liners and boundaries in low-order modeling of thermoacoustic instabilities. *Journal of Computational Physics* 2021; 428.
3. Staffelbach G, Gicquel LY, Boudier G et al. Large Eddy Simulation of self excited azimuthal modes in annular combustors. *Proceedings of the Combustion Institute* 2009; 32 II(2): 2909–2916.
4. Wolf P, Staffelbach G, Gicquel LY et al. Acoustic and Large Eddy Simulation studies of azimuthal modes in annular combustion chambers. *Combustion and Flame* 2012; 159(11): 3398–3413.
5. Ghani A, Poinsot T, Gicquel L et al. LES of longitudinal and transverse self-excited combustion instabilities in a bluff-body stabilized turbulent premixed flame. *Combustion and Flame* 2015; 162(11): 4075–4083.
6. Juniper MP and Sujith R. Sensitivity and Nonlinearity of Thermoacoustic Oscillations. *Annual Review of Fluid Mechanics* 2018; 50(1).
7. Poinsot T. Prediction and control of combustion instabilities in real engines. *Proceedings of the Combustion Institute* 2017; 36(1): 1–28.
8. Nicoud F, Benoit L, Sensiau C et al. Acoustic modes in combustors with complex impedances and multidimensional active flames. *AIAA Journal* 2007; 45(2).
9. Bauerheim M, Parmentier JF, Salas P et al. An analytical model for azimuthal thermoacoustic modes in an annular chamber fed by an annular plenum. *Combustion and Flame* 2014; 161(5): 1374–1389.
10. Han X, Li J and Morgans AS. Prediction of combustion instability limit cycle oscillations by combining flame describing function simulations with a thermoacoustic network model. *Combustion and Flame* 2015; 162: 3632–3647.
11. Li J, Yang D, Luzzato C et al. Open Source Combustion Instability Low Order Simulator (OSCILOS-Long) Technical report. Technical report, Department of Mechanical Engineering, Imperial College London, UK, 2017.
12. Emmert T, Meindl M, Jaensch S et al. Linear state space interconnect modeling of acoustic systems. *Acta Acustica united with Acustica* 2016; 102(5): 824–833.
13. Schuermans B, Bellucci V and Paschereit CO. Thermoacoustic modeling and control of multi burner combustion systems. *American Society of Mechanical Engineers, International Gas Turbine Institute, Turbo Expo (Publication) IGTI* 2003; 2: 509–519.
14. Bethke S, Wever U and Krebs W. Stability analysis of gas-turbine combustion chamber. In *11th AIAA/CEAS Aeroacoustics Conference*, volume 1. ISBN 1563477300, pp. 407–422.
15. Schuermans B, Guethe F, Pennell D et al. Thermoacoustic modeling of a gas turbine using transfer functions measured under full engine pressure. *Journal of Engineering for Gas Turbines and Power* 2010; 132(11).
16. Stow SR and Dowling AP. A Time-Domain Network Model for Nonlinear Thermoacoustic Oscillations. *Journal of Engineering for Gas Turbines and Power* 2009; 131(3): 031502.
17. Bauerheim M, Nicoud F and Poinsot T. Progress in analytical methods to predict and control azimuthal combustion instability modes in annular chambers. *Physics of Fluids* 2016; 28(2).
18. Noiray N and Schuermans B. On the dynamic nature of azimuthal thermoacoustic modes in annular gas turbine combustion chambers. In *Proceedings of the Royal Society A*.
19. Ghirardo G, Juniper MP and Moeck JP. Weakly nonlinear analysis of thermoacoustic instabilities in annular combustors. *Journal of Fluid Mechanics* 2016; 805: 52–87.
20. Yang D, Laera D and Morgans AS. A systematic study of nonlinear coupling of thermoacoustic modes in annular combustors. *Journal of Sound and Vibration* 2019; 456: 137–161.
21. Orchini A, Mensah GA and Moeck JP. Effects of nonlinear modal interactions on the thermoacoustic stability of annular combustors. *Journal of Engineering for Gas Turbines and Power* 2019; 141(2).
22. Bellucci V, Schuermans B, Nowak D et al. Thermoacoustic modeling of a gas turbine combustor equipped with acoustic dampers. *Journal of Turbomachinery* 2005; 127(2): 372–379.
23. Bothien M, Noiray N and Schuermans B. Analysis of azimuthal thermoacoustic modes in annular gas turbine combustion chambers. *Journal of Engineering for Gas Turbines and Power* 2015; 137(June 2015): 1–8.
24. Meindl M, Albayrak A and Polifke W. A state-space formulation of a discontinuous Galerkin method for thermoacoustic stability analysis. *Journal of Sound and Vibration* 2020; 481: 1–21.
25. Gullaud E and Nicoud F. Effect of Perforated Plates on the Acoustics of Annular Combustors. *AIAA Journal* 2012; 50(12): 2629–2642.
26. Douasbin Q, Scalo C, Selle L et al. Delayed-time domain impedance boundary conditions (D-TDIBC). *Journal of Computational Physics* 2018; 371: 50–66.
27. Gustavsen B and Semlyen A. Rational approximation of frequency domain responses by vector fitting. *IEEE Transactions on Power Delivery* 1999; 14(3).
28. Buschmann PE, Mensah GA, Nicoud F et al. Solution of Thermoacoustic Eigenvalue Problems With a Noniterative Method. *Journal of Engineering for Gas Turbines and Power* 2020; 142(3).
29. Mensah GA, Campa G and Moeck JP. Efficient Computation of Thermoacoustic Modes in Industrial Annular Combustion Chambers Based on Bloch-Wave Theory. *Journal of Engineering for Gas Turbines and Power* 2016; 138(8).
30. Motheau E, Nicoud F and Poinsot T. Mixed acoustic-entropy combustion instabilities in gas turbines. *Journal of Fluid Mechanics* 2014; 749: 542–576.
31. Magri L. Adjoint Methods as Design Tools in Thermoacoustics. *Applied Mechanics Reviews* 2019; 71(2).